Influence of a strong magnetic field on the hydrogen molecular ion using B-spline-type basis-sets*

Zhang Yue-Xia(张月霞)† and Zhang Xiao-Long(张小龙)

Department of Physics, Chongqing University, Chongqing 400044, *China*

(Received 18 July 2015; revised manuscript received 19 August 2015; published online 20 October 2015)

As an improvement on our previous work [*J. Phys. B: At. Mol. Opt. Phys.* **45** 085101 (2012)], an accurate method combining the spheroidal coordinates and B-spline basis is applied to study the ground state $1\sigma_g$ and low excited states $1\sigma_u, 1\pi_{g,u}, 1\delta_{g,u}, 2\sigma_g$ of the H_2^+ in magnetic fields ranging from 10^9 Gs (1 Gs = 10^{-4} T) to 4.414×10^{13} Gs. Comparing the one-center method used in our previous work, the present method has a higher precision with a shorter computing time. Equilibrium distances of the states of the H_2^+ in strong magnetic fields were found to be accurate to 3∼5 significant digits (s.d.) and the total energies 6∼11 s.d., even for some antibonding state, such as $1\pi_g$, which is difficult for the one-center method to give reliable results while the field strength is $B \geq 10^{13}$ Gs. For the large disagreement in previous works, such as the equilibrium distances of the $1\pi_g$ state at $B = 10^9$ Gs, the present data may be used as a reference. Further, the potential energy curves (PECs) and the electronic probability density distributions (EPDDs) of the bound states $1\sigma_g$, $1\pi_u$, $1\delta_g$ and antibonding states $1\sigma_u$, $1\pi_g$, $1\delta_u$ for $B = 1$, 10, 100, 1000 a.u. (atomic unit) are compared, so that the different influences of the magnetic fields on the chemical bonds of the bound states and antibonding states are discussed in detail.

Keywords: magnetic field, B-spline, hydrogen molecular ion

PACS: 31.10.+z, 31.15.–p, 31.15.ac **DOI:** 10.1088/1674-1056/24/12/123101

1. Introduction

In our previous paper,[1] the one-center method is applied to study the ground state $1\sigma_g$ and low-lying states $1\sigma_u$, $1\pi_{g,u}$, $1\delta_{g,u}$, and $2\sigma_g$ for the H_2^+ within the magnetic field region 10^9 Gs$\leq B \leq 4.414\times10^{13}$ Gs. The goal of the study has two parts. One is to solve the slow convergence problem existing in the one-center method, which is solved successfully and high-precision energies can be comparable to those obtained by multicenter methods. The other is to study states in all fields regions, which is different from most methods referring to the partial region,[2–10] except the trial function method.[11–13] The B-spline basis plays a critical role in the paper. While the results with high precision are at the cost of the large matrix of the basis. So for some antibonding state, such as $1\pi_g$, it is difficult to get results for $B > 1000$ a.u. using the one-center method. The difficulty of the calculation leads to that only the energies and the equilibrium distances in different magnetic fields can be studied.

Obviously, the results in Ref. [1] are not sufficient for studying the influence of the magnetic fields for the chemical bond of the states of H_2^+.[14,15] The main problem that needs to be solved is to optimize the one-center method. As a test, we combined the spheroidal coordinates and B-spline basis to calculate the equilibrium distance and the total energies of the states with $|m| \leq 4$ for $B = 1$ a.u. in Ref. [16]. An accuracy from 10^{-9}–10^{-12} can be obtained for the energies when $|m| \leq 3$.

The purpose of this paper is to optimize the method in Ref. [1] and Ref. [16] and investigate the influence of the magnetic field on the chemical bond. In this paper, the total energies and equilibrium distances of the ground states $1\sigma_{g,u}$, $1\pi_{g,u}$, $1\delta_{g,u}$, $2\sigma_g$ in all the field regions are recalculated. It is helpful for us to learn the advantage of the present method and narrow the gap between different methods. Next, the potential energy curves and the electronic probability density distributions of the states $1\sigma_{g,u}$, $1\pi_{g,u}$, $1\delta_{g,u}$ for a large region of $B = 1$, 10, 100, 1000 a.u. are plotted. Because the influence of the magnetic fields on the chemical bonds of the bound states and the antibonding states is different, so they are compared and discussed in detail.

2. Method

As shown in Fig. 1, r_1 and r_2 represent the distances from the electron to proton 1 and proton 2, respectively, R is the internuclear distance, and there is a constant magnetic field along the z axis. The electronic Hamiltonian of H_2^+ within the Born–Oppenheimer approximation is given by

$$H = -\frac{1}{2}\nabla^2 - \frac{1}{r_1} - \frac{1}{r_2} + \frac{1}{R} + \frac{1}{2}\gamma\hat{L}_z + \frac{1}{8}\gamma^2\rho^2, \qquad (1)$$

where $\hat{L}_z$ is the z component of angular momentum and the magnetic field strength $\gamma = B/B_0$, $B_0 = 2.35\times10^5$ T. The

*Project supported by the National Natural Science Foundation of China (Grant No. 11204389) and the Natural Science Foundation Project of Chongqing (Grant Nos. CSTC2012jjA50015 and CSTC2012jjA00012).

†Corresponding author. E-mail: zyuex02@cqu.edu.cn

© 2015 Chinese Physical Society and IOP Publishing Ltd

atomic units (a.u.) are used in the present study unless specifically stated. Moreover, ρ is the transversal distance,[3] which can be written as

$$\rho = \frac{1}{2R}\sqrt{[(r_1+r_2)^2-R^2][R^2-(r_1-r_2)^2]}.$$

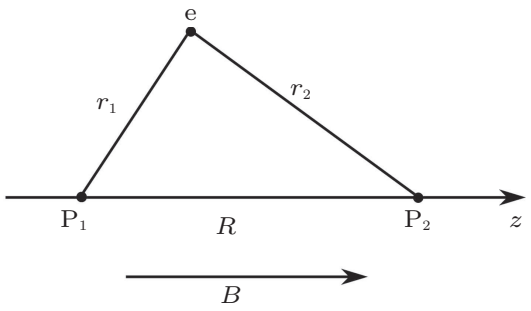


Fig. 1. Model of the H_2^+ in the magnetic fields along the z axis.

In the case of a parallel magnetic field, the Hamiltonian of H_2^+ is cylindrically symmetric, so that the magnetic quantum number m is conserved and the axial wave function $\exp(\mathrm{i}m\phi)/\sqrt{2\pi}$ can be factored out. The spheroidal coordinate has been proved as a good choice for the system with cylindrical symmetry in many literatures and will be used in the present paper. If we use two variables, u and v, which satisfy:

$$u = (r_1+r_2)/R,\ u \in [1,\infty]$$

and

$$v = (r_1-r_2)/R,\ v \in [-1,1],$$

to replace r_1 and r_2 in Eq. (1), then the Hamiltonian for a given m in spheroidal coordinates can be read as follows:

$$H = H_{\mathrm{T}} + H_{\mathrm{C}} + H_{\mathrm{M}}, \tag{2}$$

with

$$\begin{aligned} H_{\mathrm{T}} =& -\frac{2}{R^2(u^2-v^2)}\left[\frac{\partial}{\partial u}(u^2-1)\frac{\partial}{\partial u}\right. \\ &\left.+\frac{\partial}{\partial v}(1-v^2)\frac{\partial}{\partial v}-\frac{m^2(u^2-v^2)}{(u^2-1)(1-v^2)}\right], \\ H_{\mathrm{C}} =& -\frac{2}{R}\left(\frac{1}{u+v}+\frac{1}{u-v}\right)+\frac{1}{R}, \end{aligned} \tag{3}$$

and

$$H_{\mathrm{M}} = \frac{\gamma}{2}m+\frac{\gamma^2R^2}{32}(u^2-1)(1-v^2)$$

being the kinetic, Coulomb interaction, and magnetic field terms, respectively. Comparing the H_{C} term with that in spherical coordinates, which is

$$-2\sum_{\lambda=0(\mathrm{even})}^{\infty}\frac{r_<^\lambda}{r_>^{\lambda+1}}P_\lambda(\xi)$$

in Ref. [1], the expression in Eq. (3) is much more simple. In other words, the present method avoids the complicated numerical calculation on the singularities at the nuclear positions of H_2^+, which must be considered in the one-center method. Thus a large amount of time can be saved in the present computation.

The wavefunction of the system is expanded in symmetric B-spline type basis set as follows:[17,18]

$$\Psi(u,v) = \sum_{i=1}^{N_{\mathrm{u}}}\sum_{j=1}^{N_v} C_{ij}(u^2-1)^{|m|/2}(1-v^2)^{|m|/2}\Phi_{ij}(u,v), \tag{4}$$

with

$$\Phi_{ij}(u,v) = B_i^{k_{\mathrm{u}}}(u)[B_j^{k_v}(v)+\pi B_{2N_v+1-j}^{k_v}(v)]. \tag{5}$$

Here, k_{u} and N_{u} denote the order and the number of B-spline basis function along the u axis. Similarly, k_v and N_v along the v axis. π is the parity quantum number, and $\pi = \pm 1$ represent even and odd states, respectively. It is worth mentioning that only half of the basis set is needed using the symmetric form in Eq. (5) comparing with the general B-spline basis in Ref. [19]. It is a very effective way to reduce the amount of calculation and speed up the convergence in the present method.

In addition, a proper knot sequence is also important for speeding up the convergence. In this project, the u axis knot sequence $\{u_k\}$ can be written as follows:

$$\begin{aligned} 1 = u_1 = u_2 = \cdots = u_{k_{\mathrm{u}}} \le u_{k_{\mathrm{u}}+1} \\ \le u_{N_{\mathrm{u}}+k_{\mathrm{u}}-2} \le u_{N_{\mathrm{u}}+k_{\mathrm{u}}-1} \le u_{N_{\mathrm{u}}+k_{\mathrm{u}}} = u_{\max}. \end{aligned}$$

The knots in the domain $[1,u_{\max}]$ are distributed exponentially as follows:

$$u_i = 1+(u_{\max}-1)\frac{\mathrm{e}^{\lambda(i-1)}-1}{\mathrm{e}^{\lambda(N_{\mathrm{u}}-k_{\mathrm{u}})}-1},\ \lambda = \frac{\alpha\times(u_{\max}-1)}{(N_{\mathrm{u}}-k_{\mathrm{u}}+1)}. \tag{6}$$

Here, subscript i values from $[1,N_{\mathrm{u}}-k_{\mathrm{u}}+1]$ and α is an adjustable parameter.

The v axis knot sequence $\{v_j\}$ can be written as follows:

$$\begin{aligned} -1 = v_1 = v_2 = \cdots = v_{k_v} \le v_{k_v+1} \le \cdots v_j \le \cdots \\ \le v_{N_v+1} = v_{N_v+2} = \cdots = v_{N_v+k_v} = 1. \end{aligned}$$

The knot distribution in the domain $[-1,1]$ is regarded as a cosine function with

$$v_j = -\cos\left[\frac{j-k_v}{N_v-k_v+1}\pi\right],\ j \in [k_v, N_v+1].$$

The knot distribution using the cosine function is more effective for speeding up the convergence than that in Ref. [16], where it is uniform. For example the $1\pi_{\mathrm{g}}$ state at $B = 1$ a.u. shown in the following Table 4, $80\times 60(N_{\mathrm{u}}\times N_v)$ basis is needed in Ref. [16], while $60\times 40(N_{\mathrm{u}}\times N_v)$ basis is enough

to obtain the same results in this paper. For more detailed discussions about the knots and the properties of B-splines, readers can refer to Refs. [1], [20]–[23]. The eigenvalues and the corresponding wave functions of electronic states are obtained by diagonalization of the effective Hamiltonian (2) in a space spanned by the basis functions (4).

3. Results and discussion

3.1. The equilibrium distances and the total energies

In the following, the equilibrium distances and total energies for the states $1\sigma_{g,u}$, $1\pi_{g,u}$, $1\delta_{g,u}$, and $2\sigma_g$ of H_2^+ for 10^9 Gs$\leq B \leq 4.414\times10^{13}$ Gs are given and compared to other results in several tables. In calculations, we fix the parameter $u_{max} = 40$ and the number of B-spline basis along the u-axis $N_u = 60$. So in fact, only two parameters, α in Eq. (6) and the number of B-spline basis along the v-axis N_v need to be adjusted. The detailed numbers N_u and N_v of the B-spline basis for every state in different magnetic fields have been listed in the corresponding tables. It is worth mentioning that the calculation time is significantly reduced compared to that taken by the one-center method in Ref. [1]. For example, for the $1\sigma_g$ state at $B = 4.414\times10^{13}$ Gs in Table 1, only 4 minutes are needed in the present paper, while one and a half hours were used in Ref. [1]. Even for the $2\sigma_g$ state at $B = 4.414\times10^{13}$ Gs in Table 7, the number of the basis $N_u \times N_v = 60\times700$ is the largest in the present paper, about 40 minutes are needed.

3.1.1. $1\sigma_g$ state ($m = 0$, even parity)

Table 1 lists the equilibrium distances R_{eq} and total energies E_T for the ground state $1\sigma_g$ of H_2^+ in different magnetic fields. Compared with the data given by Guan in Refs. [3] and [24] in fields with strengths below 2.35×10^{10} Gs, the equilibrium distances and total energies obtained in the present method are in close agreement with the last digit listed by Guan. In Comparison with the results at $B = 1$, 10, 100, 1000 a.u. given by Vincke in Ref. [8], which are the most accurate found in the literature, the equilibrium distances are consistent with each other at least 5 s.d. and the total energies at least 11 s.d. Compared with previous results obtained by the one-center method in Ref. [1], the precision of the total energies is improved obviously, though the computation time is reduced largely. That shows the spheroidal coordinates are more suitable than the spherical coordinates for studying H_2^+ in all the field regions from 10^9 Gs to 4.414×10^{13} Gs. The accuracy of the equilibrium distances is estimated at least about 4 s.d. and that of the total energies about 7∼11 s.d. The case is the same as other literatures, the equilibrium distances decrease and the total energies increase as the magnetic field strength increases. This means that the states are increasingly stable as the strength of the magnetic field increases.

Table 1. The equilibrium distances R_{eq} and total energies E_T for the ground state $1\sigma_g$ of H_2^+ in different magnetic fields, are here compared to those calculated using other methods.

B/Gs	N_u	N_v	$R_{eq}^{[Ref.]}$	$E_T^{[Ref.]}$
10^9	60	25	1.9234	−1.150717897
	50	30	1.9234[1]	−1.15071723[1]
			1.923[12,13]	−1.15070[12,13]
			1.924[2]	−1.150718[2]
			1.9233[25]	−1.15072[25]
			1.9234[24]	−1.150717898[24]
2.35×10^9	60	25	1.7520828	−0.94997649055
	110	85	1.7520[1]	−0.94997644[1]
			1.752[12,13]	−0.94992[12,13]
			1.76[6]	−0.94642[6]
			1.7521[3]	−0.94997649[3]
			1.7520838[8]	−0.94997649055[8]
10^{10}	60	25	1.2464	1.090302124
	50	30	1.2465[1]	1.0903028[1]
			1.246[12,13]	1.09044[12,13]
			1.246[2]	1.090308[2]
			1.2464[25]	1.08979[25]
			1.2464[24]	1.090302124[24]
2.35×10^{10}	60	25	0.9570223	5.650027927964
	80	50	0.9570[1]	5.6500282[1]
			0.957 ± 0.002[12,13]	5.65024[12,13]
			0.950[2]	5.65[2]
			0.958[26]	5.65[26]
			0.957[3]	5.650028[3]
			0.9570236[8]	5.650027927964[8]
10^{11}	60	25	0.5933	35.042574
	80	50	0.5917[1]	35.042670[1]
			0.593 ± 0.001[12,13]	35.0432[12,13]
			0.593[2]	35.0428[2]
2.35×10^{11}	60	50	0.447793	89.707837077
	80	50	0.4472[1]	89.707803[1]
			0.448 ± 0.001[12,13]	89.7090[12,13]
			0.446[2]	89.7108[2]
			0.448[26]	89.720[26]
			0.447794[8]	89.707837077[8]
10^{12}	60	50	0.2834	408.387298
	80	50	0.2832[1]	408.38719[1]
			0.283 ± 0.001[12,13]	408.3894[12,13]
			0.28[27]	408.4731[27]
2.35×10^{12}	60	100	0.219783	977.21833022
	80	50	0.2198[1]	977.21835[1]
			0.2197 ± 0.0005[12,13]	977.2214[12,13]
			0.219783[8]	977.21833022[8]
10^{13}	60	100	0.1472	4219.5588
	160	100	0.1472[1]	4219.559[1]
			0.1472 ± 0.0002[12,13]	4219.565[12,13]
			0.15[27]	4219.58[27]
2.35×10^{13}	60	200	0.1183	9954.1948
	160	100	0.1183[1]	9954.195[1]
			0.1183 ± 0.0002[12,13]	9954.203[12,13]
4.414×10^{13}	60	200	0.1016	18728.4675
	160	100	0.1016[1]	18728.468[1]
			0.1016 ± 0.0002[12,13]	18728.477[12,13]

3.1.2. $1\sigma_u$ state ($m=0$, odd parity)

As shown in Table 1, the equilibrium distances R_{eq} and the total energies E_T for the $1\sigma_u$ state in magnetic fields with different strengths are listed in Table 2. Most of the calculations on the $1\sigma_u$ state are concentrated on the domain $B \leq 10^{10}$ Gs as shown in Table 2. For the cases of $B > 10^{10}$ Gs, there are two calculations, i.e., one by Turbiner[12,13] and the other by us using the one-center method,[1] available. In the same way as in the case of $1\sigma_g$, the calculated equilibrium distances and total energies of the state $1\sigma_u$ in the present method are closer to the data listed by Guan[3,24] for 10^9 Gs$\leq B \leq 10^{10}$ Gs and Vincke at $B = 2.35 \times 10^9$ Gs than those obtained in the one-center method.[1] Results in the present method agree with the last digit given by Guan and Vincke. For 2.35×10^{10} Gs$\leq B \leq 10^{13}$ Gs, the results are closer to the data obtained by us in the one-center method[1] than Turbiner,[11] including the equilibrium distance and the total energy at $B = 2.35 \times 10^{10}$ Gs, where there is a larger difference between them. For the equilibrium distance from $B = 2.35 \times 10^{13}$ Gs, our data 2.143 is closer in agreement with 2.134 given by Turbiner than 2.02 by the one-center method. Also for $B = 4.414 \times 10^{13}$ Gs, there are no data available using the one-center method. However, the results of the present method are in good agreement with Turbiner's; this shows that this method is more suitable for H_2^+ than the one-center method even at magnetic field strengths reaching 4.414×10^{13} Gs. The accuracy of the equilibrium distances is estimated at about 2∼5 s.d. and the total energies about 7∼11 s.d.

Table 2. Equilibrium distances R_{eq} and total energies E_T for the excited state $1\sigma_u$.

B/Gs	N_u	N_v	$R_{eq}^{[Ref.]}$	$E_T^{[Ref.]}$
10^9	60	25	11.097	−0.921096088
	240	140	11.074[1]	−0.92108946[1]
			11.19[12,13]	−0.92103[12,13]
			11.097[24]	−0.92109608[24]
			11.039[25]	−0.92063[25]
2.35×10^9	60	25	9.58768	−0.66287291463
	240	140	9.580[1]	−0.6628674[1]
			9.73[12,13]	−0.66271[12,13]
			9.588[3]	−0.66287292[3]
			9.6[6]	−0.66[6]
			9.58768[8]	−0.66287291463[8]
10^{10}	60	25	7.1392	1.638944317
	240	140	7.1357[1]	1.6389499[1]
			7.18[12,13]	1.63989[12,13]
			7.139[24]	1.63894432[24]
2.35×10^{10}	60	25	6.0217	6.5027272
	240	120	6.0192[1]	6.5027344[1]
			6.336[12,13]	6.52362[12,13]
10^{11}	60	50	4.6163	36.83148
	280	100	4.6123[1]	36.8315[1]
			4.629[12,13]	36.8367[12,13]
2.35×10^{11}	60	50	4.001	92.41778
	320	100	3.996[1]	92.4178[1]
			3.976[12,13]	92.4257[12,13]
10^{12}	60	100	3.208	413.60514
	280	120	3.2108[1]	413.605[1]
			3.209[12,13]	413.6175[12,13]
2.35×10^{12}	60	100	2.848	984.6719
	350	120	2.835[1]	984.672[1]
			2.862[12,13]	984.6852[12,13]
10^{13}	60	200	2.368	4232.5419
	350	120	2.344[1]	4232.54[1]
			2.360[12,13]	4232.554[12,13]
2.35×10^{13}	60	400	2.143	9971.7143
	240	155	2.02[1]	9971.72[1]
			2.134[12,13]	9971.727[12,13]
4.414×10^{13}	60	400	1.998	18750.0521
			2.021[12,13]	18750.07[12,13]

Comparing the numbers of the basis ($N_u \times N_v$) for $1\sigma_u$ and $1\sigma_g$, the amount of computation for $1\sigma_u$ increases obviously; this may refer to the antibonding behavior of the $1\sigma_u$ state. It can also explain why less works are found for the $1\sigma_u$ state than the $1\sigma_g$ state. Table 2 also shows the equilibrium distances R_{eq} decreasing and total energies E_T of the $1\sigma_u$ state increasing as the magnetic field grows from 10^9 Gs to 4.414×10^{13} Gs.

3.1.3. $1\pi_u$ state ($m=-1$, even parity)

We compared the equilibrium distances R_{eq} and total energies E_T for the excited state $1\pi_u$ using different methods within a magnetic field ranging from 10^9 Gs to 4.414×10^{13} Gs as shown in Table 3. The present results are in perfect agreement with the data obtained by Guan in Refs. [3] and [24], Vincke in Ref. [11], and us using the one-center method in Ref. [1]. Even for $B = 4.414 \times 10^{13}$ Gs, the results of the present method are very consistent with those in the one-center method. Turbiner also gave the equilibrium distances R_{eq} and total energies E_T with the field strength from 10^9 Gs to 4.414×10^{13} Gs. Their values are less accurate, but they are also closely consistent with our data.

We compare the energies of the $1\pi_u$ state in Table 3 with those of the $1\sigma_u$ state in Table 2, and the energy crossing is implied in the range 10^{12} Gs$< B < 2.35 \times 10^{12}$ Gs.

3.1.4. $1\pi_g$ state ($m=-1$, odd parity)

In Table 4, the results of the antibonding state $1\pi_g$ in different literatures are listed. The equilibrium distances of the $1\pi_g$ were found to be larger than those of the antibonding state $1\sigma_u$. As shown in Table 4, most works focus on the case for $B = 2.35 \times 10^9$ Gs. Compared with the high-precision results given by Vincke in Ref. [8], the equilibrium distance is in agreement within 5 s.d. and the total energy within 11 s.d. For $B = 10^9$ Gs, the equilibrium distances listed in Ref. [1] and Refs. [12] and [13] are 18.08 and 20.10, respectively. The result in the present paper is in good agreement with that using the one-center method in Ref. [1]. For 10^{10} Gs$\leq B \leq 2.35 \times 10^{12}$ Gs, two sets of data, i.e., ours using the one-center method and Turbiner's, can be used to

Table 3. Equilibrium distances R_{eq} and total energies E_T for the excited state $1\pi_u$.

B/Gs	N_u	N_v	$R_{eq}^{[Ref.]}$	$E_T^{[Ref.]}$
10^9	60	25	4.9375	−0.293629861
	50	30	4.9378[1]	−0.29362986[1]
			4.940[12,13]	−0.293592[12,13]
			4.9375[24]	−0.293629862[24]
2.35×10^9	60	25	3.677025	−0.0202355799557
	110	85	3.67695[1]	−0.020235580[1]
			3.676[12,13]	−0.020150[12,13]
			3.6769[3]	−0.02023558[3]
			3.68[6]	−0.02014[6]
			3.677022[8]	−0.020235579956[8]
10^{10}	60	25	2.1271	2.37079164
	50	30	2.127[1]	2.3707916[1]
			2.130[12,13]	2.371845[12,13]
2.35×10^{10}	60	25	1.5306	7.29525174
	80	50	1.5311[1]	7.2952518[1]
			1.526[12,13]	7.29682[12,13]
			1.510[2]	7.2954[2]
			1.510[28]	7.3138[28]
10^{11}	60	25	0.8864	37.6397806
	80	50	0.8869[1]	37.639779[1]
			0.887[12,13]	37.6490[12,13]
2.35×10^{11}	60	50	0.6502	93.104752
	80	50	0.6500[1]	93.104749[1]
			0.651[12,13]	93.1127[12,13]
			0.645[2]	93.1452[2]
			0.645[28]	93.1226[28]
10^{12}	60	50	0.3954	413.62475
	80	50	0.3954[1]	413.62476[1]
			0.395[12,13]	413.6306[12,13]
2.35×10^{12}	60	100	0.3002	983.86085
	80	50	0.3003[1]	983.86088[1]
			0.301[12,13]	983.874[12,13]
10^{13}	60	100	0.1946	4229.164
	160	100	0.1946[1]	4229.164[1]
			0.195[12,13]	4229.183[12,13]
2.35×10^{13}	60	100	0.1536	9965.896
	160	100	0.1536[1]	9965.896[1]
			9965.932[12,13]	
4.414×10^{13}	60	100	0.1302	18741.878
	160	100	0.1302[1]	18741.88[1]
			0.130[12,13]	18741.89[12,13]

Table 4. Equilibrium distances R_{eq} and total energies E_T for the excited state $1\pi_g$.

B/Gs	N_u	N_v	$R_{eq}^{[Ref.]}$	$E_T^{[Ref.]}$
10^9	60	25	18.08	−0.23229265
	160	100	18.08[1]	−0.23229266[1]
			20.10[12,13]	−0.232060[12,13]
2.35×10^9	60	40	13.6573	0.086399699276
	160	140	13.657[1]	0.086399692[1]
			14.05[12,13]	0.086868[12,13]
			13.66[3]	0.0863997[3]
			13.535[29]	0.101692[29]
			13.5[6]	0.0866[6]
			13.6572[8]	0.086399699286[8]
10^{10}	60	50	9.256	2.6398330
	160	140	9.257[1]	2.6398330[1]
			9.370[12,13]	2.641122[12,13]
2.35×10^{10}	60	50	7.5759	7.7476346
	240	120	7.577[1]	7.7476343[1]
			7.622[12,13]	7.749819[12,13]
10^{11}	60	50	5.605	38.672041
	240	120	5.605[1]	38.672041[1]
			5.622[12,13]	38.67642[12,13]
2.35×10^{11}	60	100	4.7808	94.728054
	240	140	4.781[1]	94.728053[1]
			4.791[12,13]	94.73386[12,13]
10^{12}	60	100	3.747	416.927258
	240	140	3.749[1]	416.927253[1]
			3.767[12,13]	416.9354[12,13]
2.35×10^{12}	60	200	3.288	988.72012
	300	140	3.292[1]	988.72010[1]
			3.321[12,13]	988.7286[12,13]
10^{13}	60	200	2.6895	4238.030
			2.708[12,13]	4238.038[12,13]
2.35×10^{13}	60	300	2.413	9978.166
			2.420[12,13]	9978.175[12,13]
4.414×10^{13}	60	400	2.219	18757.264
			2.237[12,13]	18757.273[12,13]

compare. The equilibrium distances and the total energies in the present paper are closer to those obtained by the one-center method. The accuracy of the equilibrium distance is estimated at about 3∼4 s.d. and the total energy at about 7∼8 s.d. For 10^{13} Gs$\leq B \leq 4.414\times10^{13}$ Gs, only Turbiner's data are available. They are also closely consistent with ours.

3.1.5. $1\delta_g$ state ($m=-2$, even parity)

In Table 5, the equilibrium distances R_{eq} and total energies E_T for the excited state $1\delta_g$ in strong magnetic fields are compared with the results in other literatures. Two sets of results, i.e., Turbiner's and ours obtained by using the one-center method, can be found in various magnetic fields. They agree with each other very well, especially the present results and those obtained by the one-center method, where the equilibrium distances are consistent within 3∼5 s.d. and the total energies within 6∼9 s.d., except the case for $B=2.35\times10^{12}$ Gs. For the equilibrium distance at $B=2.35\times10^{12}$ Gs, the present data 0.3533 is closer to Turbiner's 0.353 in Refs. [12] and [13] than 0.3522 obtained by the one-center method in Ref. [1].

We compared the energies of the $1\delta_g$ state to those of the $1\sigma_u$ state and $1\pi_g$ state. Two energy crossings are found, one is between the states $1\delta_g$ and $1\pi_g$ in the range from 2.35×10^{10} Gs to 10^{11} Gs, and the other between the states $1\delta_g$ and $1\sigma_u$ in the range from 10^{13} Gs to 2.35×10^{13} Gs.

3.1.6. $1\delta_u$ state ($m=-2$, odd parity)

This is another antibonding state of the H_2^+ in the free-field case. The results in different magnetic fields are listed in Table 6. For $B=2.35\times10^9$ Gs, the present equilibrium distance and the total energy are in prefect agreement with

Table 5. Equilibrium distances R_{eq} and total energies E_T for the excited state $1\delta_g$.

B/Gs	N_u	N_v	$R_{eq}^{[Ref.]}$	$E_T^{[Ref.]}$
10^9	60	25	6.868	−0.108068323
	50	30	6.868[1]	−0.108068323[1]
			6.865[12,13]	−0.107945[12,13]
2.35×10^9	60	25	4.873327	0.22109797676
	110	85	4.8733[1]	0.221097977[1]
			4.872[12,13]	0.221163[12,13]
			4.87[6]	0.22112[6]
			4.873330[8]	0.22109797675[8]
10^{10}	60	25	2.696	2.77474027
	50	30	2.696[1]	2.77474028[1]
			2.694[12,13]	2.77538[12,13]
2.35×10^{10}	60	25	1.9089	7.84994905
	80	50	1.9089[1]	7.84994907[1]
			1.907[12,13]	7.85113[12,13]
			1.880[2]	7.8504[2]
			1.880[28]	7.8694[28]
10^{11}	60	50	1.0825	38.581488
	80	50	1.0827[1]	38.581488[1]
			1.080[12,13]	38.58470[12,13]
2.35×10^{11}	60	50	0.7857	94.3746395
	80	50	0.7858[1]	94.374639[1]
			0.782[12,13]	94.38093[12,13]
			0.778[2]	94.490[2]
			0.778[28]	94.3942[28]
10^{12}	60	100	0.4697	415.66604
	80	50	0.4695[1]	415.66628[1]
			0.470[12,13]	415.6710[12,13]
2.35×10^{12}	60	100	0.3533	986.50466
	80	50	0.3522[1]	986.50928[1]
			0.353[12,13]	986.5119[12,13]
10^{13}	60	100	0.2254	4233.109
	160	100	0.2254[1]	4233.109[1]
			0.225[12,13]	4233.125[12,13]
2.35×10^{13}	60	200	0.1763	9970.781
	160	100	0.1763[1]	9970.781[1]
			0.176[12,13]	9970.802[12,13]
4.414×10^{13}	60	200	0.1485	18747.539
	160	100	0.1485[1]	18747.540[1]
			0.148[12,13]	18747.572[12,13]

those given by the one-center method in Ref. [1] and Vincke in Ref. [8]. It means the present method is also very suitable for the case of the large equilibrium distance. For 10^9 Gs$\leq B \leq 2.35\times10^{12}$ Gs, the present results have better accordance with those obtained by the one-center method in Ref. [1] than those given by Turbiner in Ref. [12] and [13]. The equilibrium distance with at least four effective figures and the energy with at least nine effective figures were consistent with the results in Ref. [1]. However, for 10^{13} Gs$\leq B \leq 4.414\times10^{13}$ Gs, the equilibrium distances have large differences from each other. The present results are larger than in another three papers.[1,12,13]

Table 6. Equilibrium distances R_{eq} and total energies E_T for the excited state $1\delta_u$.

B/Gs	N_u	N_v	$R_{eq}^{[Ref.]}$	$E_T^{[Ref.]}$
10^9	60	50	22.073	−0.068992624
	50	30	22.073[1]	−0.068992624[1]
			23.902[12,13]	−0.06873[12,13]
2.35×10^9	60	50	16.031	0.2935716431
	110	85	16.031[1]	0.2935716431[1]
			16.377[12,13]	0.29410[12,13]
			16.0[6]	0.2936[6]
			16.0309[8]	0.29357164344[8]
10^{10}	60	50	10.540	2.9681608
	120	75	10.540[1]	2.9681608[1]
			11.475[12,13]	2.97742[12,13]
2.35×10^{10}	60	50	8.5226	8.18216588
	120	75	8.5225[1]	8.18216589[1]
			9.458[12,13]	8.19892[12,13]
10^{11}	60	100	6.2026	39.36203771
	160	75	6.2024[1]	39.36203771[1]
			6.858[12,13]	39.40596[12,13]
2.35×10^{11}	60	100	5.2485	95.621353
	160	100	5.2486[1]	95.621353[1]
			5.619[12,13]	95.69542[12,13]
10^{12}	60	200	4.0675	418.267017
	160	120	4.0672[1]	418.267017[1]
			4.071[12,13]	418.4335[12,13]
2.35×10^{12}	60	200	3.549	990.386839
	200	120	3.550[1]	990.386839[1]
			3.406[12,13]	990.6416[12,13]
10^{13}	60	300	2.88	4240.3588
	160	200	2.68[1]	4240.3596[1]
			2.625[12,13]	4240.834[12,13]
2.35×10^{13}	60	300	2.57	9980.9452
	160	220	2.042[1]	9980.95742[1]
			2.391[12,13]	9981.587[12,13]
4.414×10^{13}	60	400	2.37	18760.401
	200	235	1.68[1]	18760.4473[1]
			2.230[12,13]	18761.18[12,13]

Comparing the $1\delta_u$ state in Table 4 and the $1\pi_u$ state in Table 3 at the same magnetic field strength, the equilibrium distances of the $1\delta_u$ state are larger than the $1\pi_g$ state by using the present method. It is different with Turbiner's conclusion, where for 10^{13} Gs$\leq B \leq 4.414\times10^{13}$ Gs, the equilibrium distances of the $1\delta_u$ state are smaller than those of the $1\pi_g$ state.

3.1.7. $2\sigma_g$ state ($m=0$, even parity)

In Table 7, the results of the first excited state $2\sigma_g$ for $m=0$ and even parity series are listed. The equilibrium distance of the $2\sigma_g$ state is larger than that of the ground state $1\sigma_g$. Far less investigation of this state in the $1\sigma_g$ can be found in the literature. Only Turbiner and our group used the one-center method for all magnetic fields from 10^9 Gs to 4.414×10^{13} Gs and Kappes for $B=2.35\times10^9$ Gs to investigate this state. The results obtained using different methods are consistent with each other. For example, for 10^9 Gs$\leq B \leq 10^{10}$ Gs, the

present equilibrium distances coincide exactly with the results obtained by the one-center method in Ref. [1] and the energies are in agreement with 5∼6 s.d. However, present equilibrium distances and total energies at $B = 2.35 \times 10^{13}$ Gs and 4.414×10^{13} Gs are closer to the data of Turbiner. On the other hand, the one-center method shows weakness while the magnetic field strength is very high, similar to the case of the other antibonding states $1\sigma_u$, $1\pi_g$, and $1\delta_u$.

Table 7. Equilibrium distances R_{eq} and total energies E_T for the excited state $2\sigma_g$.

B/Gs	N_u	N_v	$R_{eq}^{[Ref.]}$	$E_T^{[Ref.]}$
10^9	60	25	7.574	−0.1215213
	50	30	7.574[1]	−0.12151935[1]
			7.55[12,13]	−0.121343[12,13]
2.35×10^9	60	25	6.638	0.34895733
	110	85	6.638[1]	0.34895744[1]
			6.640[12,13]	0.34912[12,13]
			6.64[6]	0.34928[6]
10^{10}	60	25	5.199	3.3978627
	50	30	5.199[1]	3.3978636[1]
			5.2[12,13]	3.39938[12,13]
2.35×10^{10}	60	50	4.584	9.022256
	80	50	4.592[1]	9.0222549[1]
			4.6[12,13]	9.02452[12,13]
10^{11}	60	50	3.901	41.405316
	80	50	3.899[1]	41.405312[1]
			3.91[12,13]	41.4090[12,13]
2.35×10^{11}	60	75	3.653	98.77832
	80	50	3.664[1]	98.77835[1]
			3.65[12,13]	98.7822[12,13]
10^{12}	60	150	3.394	424.2256
	80	50	3.382[1]	424.2274[1]
			3.40[12,13]	424.2277[12,13]
2.35×10^{12}	60	400	3.299	998.6609
	160	140	3.299[1]	998.6609[1]
			3.30[12,13]	998.6620[12,13]
10^{13}	60	400	3.188	4253.941
	160	220	3.188[1]	4253.941[1]
			3.21[12,13]	4253.937[12,13]
2.35×10^{13}	60	500	3.140	9998.605
	160	220	3.119[1]	9998.612[1]
			3.145[12,13]	9998.608[12,13]
4.414×10^{13}	60	700	3.110	18781.572
	160	220	3.070[1]	18781.614[1]
			3.120[12,13]	18781.576[12,13]

We compared the energies of the $2\sigma_g$ state in Table 7 to those of the $1\delta_u$ state in Table 6 and the $1\delta_g$ state in Table 5. The two energies were found to cross within the range 10^9 Gs$< B < 2.35 \times 10^9$ Gs.

3.2. The potential energy curves for the states $1\sigma_{g,u}$, $1\pi_{g,u}$, and $1\delta_{g,u}$

To analyze the influence of the different magnetic fields strengths on the H_2^+ ion, the PECs of the $1\sigma_{g,u}$, $1\pi_{g,u}$, and $1\delta_{g,u}$ states in different fields strengths are compared in Fig. 2–Fig. 4. For every state, the PECs for $B = 1$, 10, 100, 1000 a.u. are chosen from bottom to top. There solid lines depict the PECs of the bound states $1\sigma_g$, $1\pi_u$, and $1\delta_g$ in different magnetic fields strengths, and dotted lines depict the antibonding states $1\sigma_u$, $1\pi_g$, and $1\delta_u$. As shown in Fig. 2–Fig. 4, with

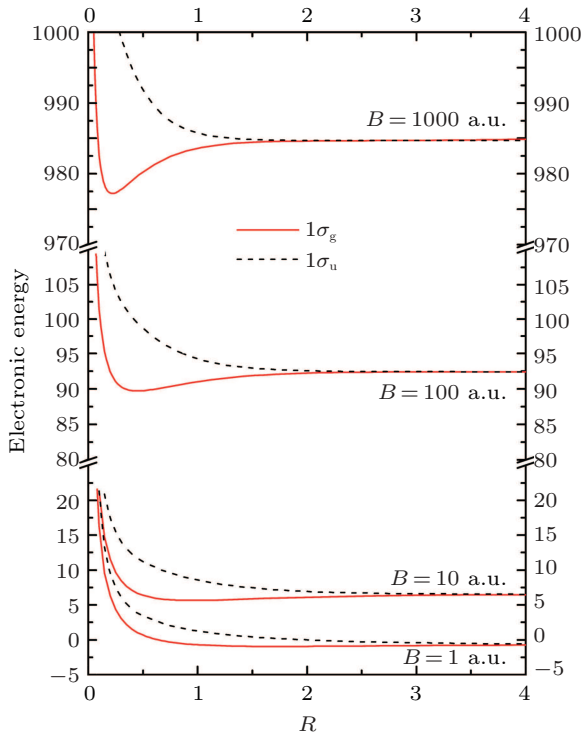


Fig. 2. (color online) The Pecs of the states $1\sigma_{g,u}$ of the H_2^+ with $B = 1$, 10, 100, 1000 a.u.

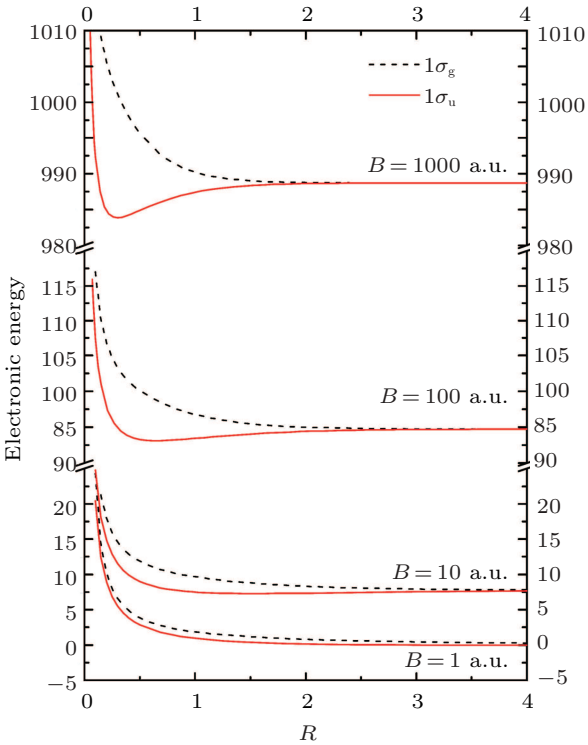


Fig. 3. (color online) The Pecs of the states $1\pi_{g,u}$ of the H_2^+ in different magnetic fields strengths.

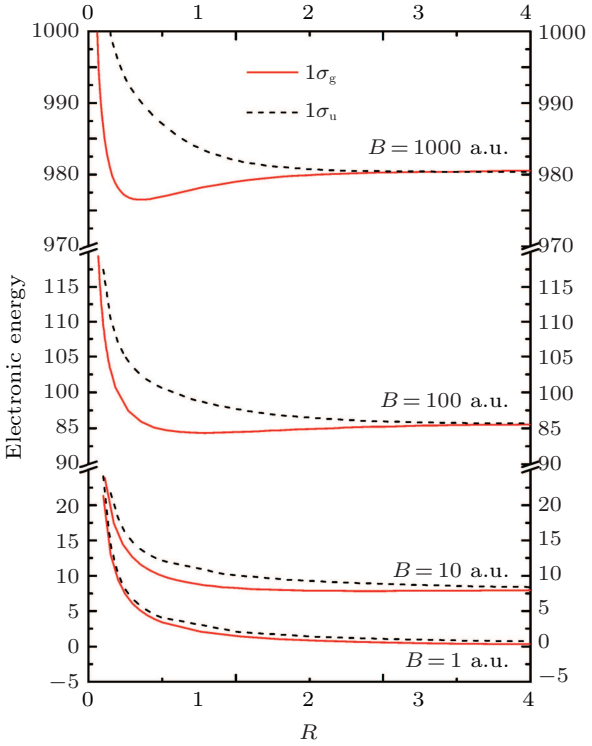


Fig. 4. (color online) The Pecs of the states $1\delta_{g,u}$ of the H_2^+ in different magnetic fields strengths.

increasing nuclear distance R, there is an overlap of the PECs between the bound state and the matching antibonding state with the same magnetic quantum number m. For example, in Fig. 2, the energies of the states $1\sigma_g$ and $1\sigma_u$ equal the energies of the state 1s of the hydrogen atom in corresponding fields strengths when the nuclear distance $R \to \infty$.

Let us first consider the PECs of the bound states, that is, $1\sigma_g$, $1\pi_u$, and $1\delta_g$ in different magnetic field strengths. A common feature can be easily found. With increasing field strength, the more pronounced potential well located corresponding equilibrium distance is shown. It means stronger attraction exists with increasing magnetic field strength. The depths of the potential well are also given quantitatively by the dissociation energies of Table 8. As expected, for every bound state, the dissociation energies increase with the fields strengths from 1 a.u. to 1000 a.u. If we estimate the influence of the magnetic field on the state according to the ratio of the dissociation energies $E_D(B)/E_D(B = 1 \text{ a.u.})$, they are 2.97, 9.43, 25.9 for the state $1\sigma_g$ in $B = 10$, 100, 1000 a.u., respectively. The ratios are 4.24, 15.2, and 45.4 for $1\pi_u$ and 4.58, 17.2, and 53.3 for $1\delta_g$. For the same magnetic field strength, the ratios of the three states $1\sigma_g$, $1\pi_u$, and $1\delta_g$ increase, such as for $B = 1000$ a.u., $25.9 < 45.4 < 53.3$. It shows the influence of the magnetic field increases with $|m|$ from 0 to 2.

Next, let us take a look at the influence of the magnetic field on the antibonding states $1\sigma_u$, $1\pi_g$, and $1\delta_u$. As depicted in dotted lines in Fig. 2–Fig. 4, a shallow potential well exists in the PECs. The depths of the potential wells, that is, the dissociation energies of Table 8, are the order of magnitude of 10^{-4} for $B = 1$ a.u. and 10^{-3} for $B > 1$ a.u. Same as the case of the bound states, dissociation energies of every antibonding state increase with the increasing magnetic field strength from 1 a.u. to 1000 a.u. The ratios of the dissociation energies $E_D(B)/E_D(B = 1 \text{ a.u.})$ are 3.13, 4.88, and 6.17 for $1\sigma_u$ state in $B = 10$, 100, 1000 a.u., respectively, and they are 3.74, 5.97, 7.48 for $1\pi_g$ and 4.23, 6.96, 8.85 for $1\delta_u$. In the same way as in the case of the bound states, the ratios increase with increasing $|m|$ for the same magnetic field strength. It means the same magnetic field strength has a greater influence on the state with larger $|m|$. For the case of the states with the same m and B, the radios are 25.9 and 6.17 for $1\sigma_g$ and $1\sigma_u$ with $B = 1000$ a.u., respectively. It is not difficult to find that the ratio of the antibonding state is much smaller than that of the corresponding bound state. The conclusion can be drawn that the same change of magnetic field strength has a smaller influence on the dissociation energies of the antibonding states than the corresponding bound states with the same m.

However, as we all known, existence of the potential well is not a criteria to judge whether a molecular bond is stable with respect to dissociation $H_2^+ \to H + p$. Only if a vibrational state can exist in the potential well, the molecular bond is stable. To the best of our knowledge, the vibrational energies are referred to in some works. For example, vibrational energies for $1\sigma_g$ with 10^9 Gs$\leq B \leq 4.414 \times 10^{13}$ Gs are given in Refs. [12] and [13], and the vibrational frequencies for $1\sigma_g$, $1\pi_u$ and $1\delta_g$ with $B \leq 10^4$ a.u. are calculated based on the one-center method in Ref. [30]. Comparing dissociation energies in Table 8 and the vibrational energies in Refs. [12], [13], and [30], we can find that the dissociation energies are larger than the corresponding vibrational energies. In every state, the differences between these two energies are larger and larger with the increasing magnetic fields. For example, for the state $1\sigma_g$

Table 8. Dissociation energies E_D of the states $1\sigma_{g,u}$, $1\pi_{g,u}$, and $1\delta_{g,u}$ of H_2^+ with $B = 1$, 10, 100, 1000 a.u. In the calculation, $E_D = E_T(H) - E_T(H_2^+)$, and $E_T(H)$ is the energy of the hydrogen atom in corresponding magnetic field. The data in Ref. [31] is used in the present paper. H_2^+ in different magnetic fields, are compared here to those calculated using other methods.

B/Gs	B/a.u.	$1\sigma_g$	$1\sigma_u$	$1\pi_u$	$1\pi_g$	$1\delta_g$	$1\delta_u$
2.35×10^9	1	0.28763869708	5.3512116×10^{-4}	0.107041463110	$4.06183878 \times 10^{-4}$	0.07280597294	3.323066×10^{-4}
2.35×10^{10}	10	0.854377744616	1.6785×10^{-3}	0.45390358	1.5207×10^{-3}	0.3336214	1.40457×10^{-3}
2.35×10^{11}	100	2.712554451	2.61×10^{-3}	1.625727	2.425×10^{-3}	1.2490260	2.313×10^{-3}
2.35×10^{12}	1000	7.45682330	3.3×10^{-3}	4.86231	3.04×10^{-3}	3.88512	2.94×10^{-3}

in $B = 1$ a.u., dissociation energy 0.28763869708 in Table 8 is larger than the vibrational energy 0.014 in Refs. [12], [13], and 0.01328 in Ref. [30]. It means that some vibrational levels can exist in the potential well of the $1\sigma_g$ for $B = 1$ a.u. and the state $1\sigma_g$ is stable. For the state $1\sigma_g$ for $B = 1000$ a.u., the dissociation energy is 7.45682330, and the vibrational energy is 0.390 in Refs. [12], [13], and 0.3588 in Ref. [30], respectively. Obviously, the difference between these two energies for $B = 1000$ a.u. is much larger than that for $B = 1$ a.u. It means the state is more stable in stronger fields. However, no vibrational energy of the antibonding state in different magnetic fields is given because of the high accuracy, which is hard to achieve. The calculation of the vibrational energy is out of this article's scope; therefore, the stability of the antibonding states in strong fields cannot efficiently be discussed in the present paper.

3.3. Electronic probability density distributions for the states $1\sigma_{g,u}$, $1\pi_{g,u}$, and $1\delta_{g,u}$

The EPDDs in the corresponding equilibrium distance R_{eq} in the x–z plane are plotted. The states from top to bottom are the bound states $1\sigma_g$, $1\pi_u$, and $1\delta_g$ in Fig. 5, and the antibonding states $1\sigma_u$, $1\pi_g$, and $1\delta_u$ in Fig. 6. The positions of the protons are labelled at the interaction points of the dotted lines along the x axis and the z axis. For every state, the density distributions for $B = 1$, 10, 100, 1000 a.u. are considered and compared from left to right in Fig. 5 and Fig. 6, which can better explain the change of the PECs with the magnetic fields strengths. For $B = 100$ a.u. and 1000 a.u., drawings of partial enlargement are placed at the upper right corner. We compare the density distributions of every state from left and right in Fig. 5 and Fig. 6, it is easy to find that the cylindrical symmetry is more obviously about the z axis with the increasing magnetic fields, and the electronic distribution is constricted in a smaller space. However, there is also different changing tendency between the bound states and the antibonding states.

First, let us discuss the change of the density distributions of the bound state $1\sigma_g$ with the magnetic fields strengths. For $B = 1$ a.u. and 10 a.u., the electron is found with a great probability in the region around the two nuclei. When the $|z|$ value between the two nuclei gets small, the probability becomes less and less and a saddle point appears at $z = 0$. When B is added to 100 a.u. and 1000 a.u., the saddle point disappears and a large density distribution of the electron occurs in the region between the two nuclei. The density distributions of the states $1\pi_u$ and $1\delta_g$ are similar. A symmetrical density distribution occurs on both sides of the z axis for $B = 1$ a.u. With the

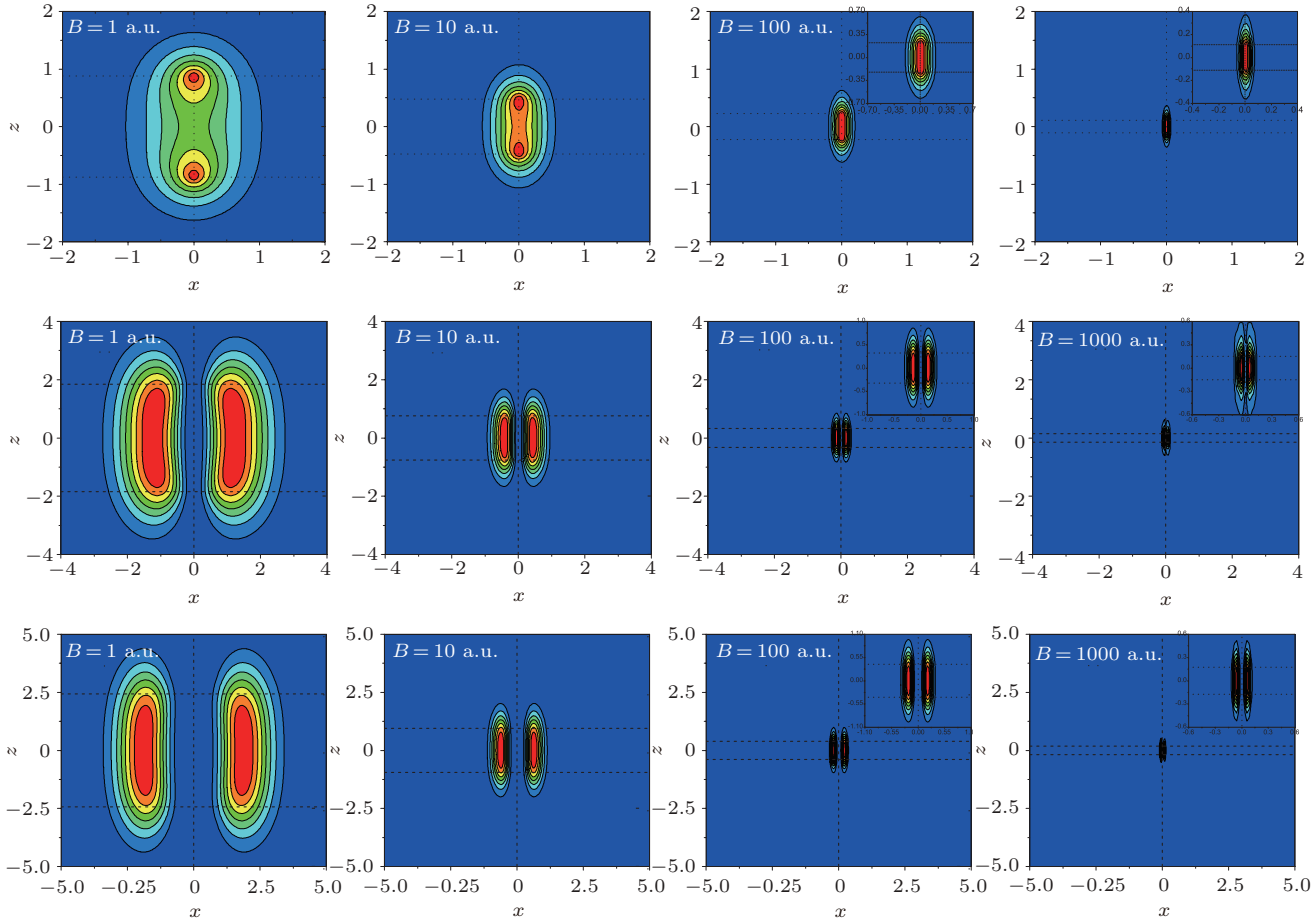


Fig. 5. (color online) The electronic probability density distributions of the bound states in the plane x–z in different magnetic fields. States from top to bottom are $1\sigma_g$, $1\pi_u$, and $1\delta_g$. The drawings of partial enlargement are placed at the upper right corner.

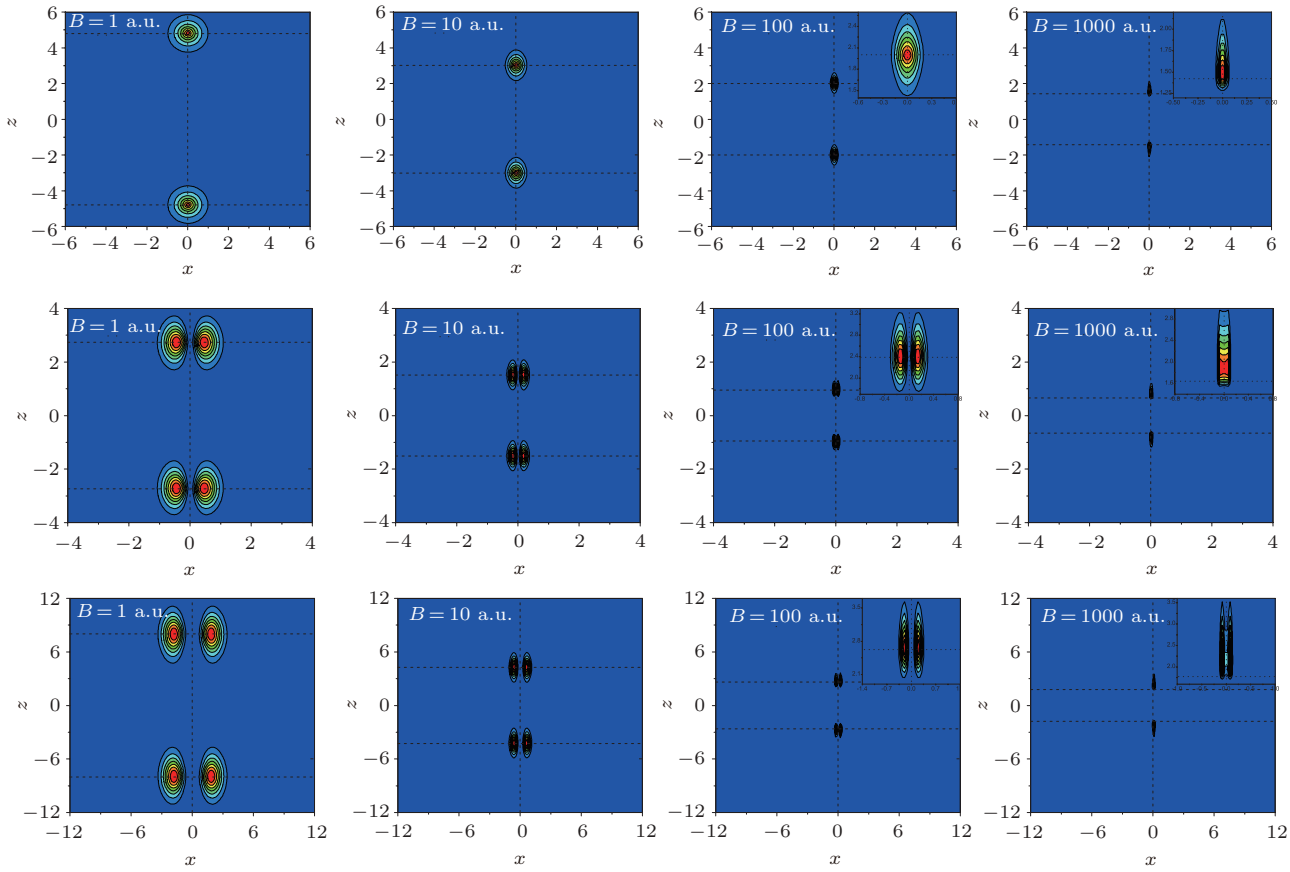


Fig. 6. (color online) The electronic probability density distributions of the antibonding states in the plane x–z in different magnetic fields. States from top to bottom are $1\sigma_u$, $1\pi_g$, and $1\delta_u$. The drawings of partial enlargement are placed at the upper right corner.

magnetic field increasing from 1 a.u. to 1000 a.u., the distance of two regions gets closer to the internuclear axis. So for $1\pi_u$ at $B = 1000$ a.u., the two regions come together. The electron can occur in the z axis with some probability. The density distribution is closer to the z axis and the increased probability between the two nuclei will screen and reduce the nucleus–nucleus repulsion. Thus, the bond length of the bound states of H_2^+ becomes shorter and shorter with the increasing magnetic fields, and the stronger attraction implies that the depth of the potential well will increase, as shown in the corresponding PECs.

The EPDDs of the antibonding states are different from those of the bound states. For example, the density distribution for $1\sigma_u$ in $B = 1$ a.u., mainly concentrate in the range of approximately $-1 < x < 1$ and $4 < |z| < 6$. There is a long range defined by $-4 < z < 4$ between the two nuclei. No electron is found. The symmetrical distribution of the electron about the positions $z = \pm R_{eq}/2$ shows the influence on the electron from the farther nucleus is a lot smaller than the nearer nucleus. With the magnetic field increasing, the distance of the two nuclei becomes shorter. Obviously the compression is the result of the effect of the magnetic field being greater than the repulsion between the two nuclei. It also shows that a stronger attraction occurs with the increasing magnetic field. However for $B = 1000$ a.u., the electronic distribution of positions $z = \pm R_{eq}/2$ becomes asymmetric. It reflects that for $B = 1000$ a.u., the effect on the electron from the nucleus farther away cannot be ignored when the distance of the two nuclei is 2.848 a.u. The density distributions of the $1\pi_g$ and $1\delta_u$ are similar. The electron mainly occurs in four regions of both sides of the z axis. With the magnetic field increasing, the region of the distribution is shrinking along the direction of parallel and perpendicular fields. For the state $1\pi_g$ in $B = 1000$ a.u., these four regions of distribution merge into two around the z axis. Similar to the case of the $1\sigma_u$ in $B = 1000$ a.u., the symmetry about the positions $z = \pm R_{eq}/2$ is also destroyed because of the effect from the nucleus farther away. The similar effect is also found for the state $1\delta_g$ in $B = 100$ a.u. and 1000 a.u. The more significant asymmetry of the density distribution for the states $1\sigma_u$, $1\pi_g$, and $1\delta_u$ for $B = 1000$ a.u. shows the relative effect of the other nucleus farther away increases with larger $|m|$ from 0 to 2.

4. Summary

In conclusion, we successfully applied the method combining the spheroidal coordinate and B-spline to calculate the equilibrium distances and the total energies of the states with $|m| \leq 2$ of H_2^+ for 10^9 Gs$\leq B \leq 4.414 \times 10^{13}$ Gs. Compared

with the one-center method used in our previous work, the present method avoids dealing with the singularities at the nuclear positions of H_2^+. So the amount of computations and time are largely reduced in the present calculation. It speeds up about 40 minutes for calculating the results of $2\sigma_g$ state of $B = 4.414 \times 10^{13}$ Gs, which is the largest base in the present calculation. However, the accuracy of the results is improved obviously in comparison with other high-precision data. The present equilibrium distances are accurate about 3 s.d.$\sim$5 s.d. and the total energies about 6 s.d.$\sim$11 s.d., even for the antibonding states $1\pi_g$, which is difficult to obtain the results for $B \geq 10^{13}$ Gs using the one-center method. Moreover, for several larger differences of the equilibrium distances between Ref. [1], Refs. [12] and [13], the present results may serve as a reference. Such as that for the $1\pi_g$ state of $B = 10^9$ Gs, the present datum 18.08 is perfectly consistent with that in Ref. [1]. However, for the $1\delta_u$ state of $B = 4.414 \times 10^{13}$ Gs, the present datum 2.38 is in closer agreement with 2.230 in Refs. [12] and [13].

Further, the PECs and dissociation energies of the bound states and the anbibonding states for $B = 1$, 10, 100, 1000 a.u. show that the depth of the potential well increases with the increasing fields strengths. The stronger behavior of the attraction is reflected for a stronger magnetic field. Comparing the corresponding vibrational energies of the bound states in Refs. [12], [13] and [30], we can find that many vibrational states can exist in the potential wells of the bound states. It means the bound states $1\sigma_g$, $1\pi_u$, $1\delta_g$ are more stable in stronger magnetic fields. However, we cannot draw a conclusion on whether antibonding states can exist stably in strong fields due the accurate vibrational energies of the antibonding states. The increasing magnetic fields can cause the electron clouds to contract along both the parallel and perpendicular magnetic fields. However, the reason is different for the bound states and the antibonding states. For the bound states, EPDDs show that more and more electrons distribute in the region between the two nuclei with increasing magnetic fields. The screening of the two nuclear charges can explain the bond lengths decreasing with stronger fields strengths. For the antibonding states, the effect of the strong magnetic field is far greater than the Coulomb repulsion between the two nuclei, which is the reason why the bond length of the antibonding states decreases with the increasing magnetic field. With the distance between two nuclei closing, the electron is also influenced by the other nucleus farther away, and the symmetry of the electron clouds on the positions $z = \pm R_{eq}/2$ changes. It is obvious for the EPDDs of the states $1\sigma_u$, $1\pi_g$ for $B = 1000$ a.u. and $1\delta_g$ for $B = 100$, 1000 a.u. The asymmetry shows also that the influence of the nucleus farther away from the electron increases with larger $|m|$ at the same magnetic field strength.

The present method can provide satisfactory results with a small amount of computation and save much computing time. The results we obtained in the present paper encourage us to extend the present method to study the influence of magnetic field strengths with different inclinations on the equilibrium distances, total energies, and molecular bonds of H_2^+. This may provide a way to better understand the spectrum of the isolated neutron star 1E1207.4-5209.

References

[1] Zhang Y X, Liu Q and Shi T Y 2012 *J. Phys. B: At. Mol. Opt. Phys.* **45** 085101
[2] Wille U 1988 *Phys. Rev. A* **38** 3210
[3] Guan X X, Li B W and Taylor K T 2003 *J. Phys. B: At. Mol. Opt. Phys.* **36** 3569
[4] Kappes U, Schmelcher P and Pacher T 1994 *Phys. Rev. A* **50** 3775
[5] Kappes U and Schmelcher P 1994 *J. Chem. Phys.* **100** 2878
[6] Kappes U and Schmelcher P 1995 *Phys. Rev. A* **51** 4542
[7] Kappes U and Schmelcher P 1996 *Phys. Rev. A* **53** 3869
[8] Vincke M and Baye D 2006 *J. Phys. B: At. Mol. Opt. Phys.* **39** 2605
[9] Kravchenko Y P and Liberman M A 1997 *Phys. Rev. A* **55** 2701
[10] Baye D, Joos de ter Beerst A and Sparenberg J M 2009 *J. Phys. B: At. Mol. Opt. Phys.* **42** 225102
[11] Turbiner A V and López Vieyra J C 2003 *Phys. Rev. A* **68** 012504
[12] Turbiner A V and López Vieyra J C 2004 *Phys. Rev. A* **69** 053413
[13] Turbiner A V and López Vieyra J C 2006 *Phys. Rep.* **424** 309
[14] Schmelcher P and Schweizer W (eds.) 1998 *Atoms and Molecules in Strong External Fields* (New York: Plenum)
[15] Sanwal D, Pavlov G G, Zavlin V E and Teter M A 2002 *Astrophys. Lett.* **574** L61
[16] Zhang Y X, Liu Q and Shi T Y 2013 *Chin. Phys. Lett.* **30** 043101
[17] Yulian V V and Alejandro S 2004 *J. Phys. B: At. Mol. Opt. Phys.* **37** 4101
[18] Zhang Y X, Kang S and Shi T Y 2008 *Chin. Phys. Lett.* **25** 3946
[19] Shi T Y, Zhang Z J and Li B W 2004 *Mod. Phys. Lett. B* **18** 113
[20] Kang S, Li J and Shi T Y 2006 *J. Phys. B: At. Mol. Opt. Phys.* **39** 3491
[21] Qiao H X and Li B W 1999 *Phys. Rev. A* **60** 3136
[22] Xi J H, Wu L J, He X H and Li B W 1992 *Phys. Rev. A* **46** 5806
[23] Shi T Y, Qiao H X and Li B W 2000 *J. Phys. B: At. Mol. Opt. Phys.* **33** L349
[24] Guan X X, Li B W and Taylor K T 2004 *J. Phys. B: At. Mol. Opt. Phys.* **37** 1985
[25] López Vieyra J C, Hess P and Turbiner A V 1997 *Phys. Rev. A* **56** 4496
[26] Larsen D M 1982 *Phys. Rev. A* **25** 1295
[27] Lai D, Salpeter E and Shapiro S L 1992 *Phys. Rev. A* **45** 4832
[28] Vincke M and Baye D 1985 *J. Phys. B: At. Mol. Opt. Phys.* **18** 167
[29] Ozaki J and Hayashi Y 1989 *J. Phys. Soc. Jpn.* **58** 3564
[30] Hu S L and Shi T Y 2013 *Chin. Phys. B* **22** 093101
[31] Baye D, Vincke M and Hesse M 2008 *J. Phys. B: At. Mol. Opt. Phys.* **41** 055005